Journal of the Geological Society, London, Vol. **161**, 2004, pp. 773–781. Printed in Great Britain.

Late Permian rifting of the South China Craton caused by the Emeishan mantle plume?

XIE-YAN SONG[1,2], MEI-FU ZHOU[1], ZHI-MIN CAO[3] & PAUL T. ROBINSON[1]
[1]*Department of Earth Sciences, University of Hong Kong, Pokfulam Road, Hong Kong, China (e-mail: xsong@hkusua.hku.hk)*
[2]*Third Department, Chengdu University of Technology, Chengdu, China*
[3]*College of Earth Sciences, Ocean University of Qingdao, Qingdao, China*

Abstract: Stratigraphic relationships and bulk-rock geochemical data indicate that Upper Permian metabasalts in the Songpan–Ganzi and Yidun terranes, on the eastern margin of the Tibetan Plateau, are part of the Emeishan large igneous province, which is believed to have formed from the Emeishan mantle plume. Eruption of the Emeishan basalts at 260 Ma was coincident with rifting of the western margin of the South China Craton to form the Songpan–Ganzi ocean basin. The spatial and temporal coincidence between basalt eruption and continental rifting, as well as regional doming prior to eruption, suggest that continental break-up was a response to the Late Permian Emeishan plume. The Songpan–Ganzi ocean basin was rapidly filled with Triassic flysch deposits, then deformed and uplifted during Mesozoic collision between the North China and South China Blocks and the Tertiary collision of India and Eurasia.

Keywords: Songpan–Ganzi, South China Craton, Emeishan basalts, Tibet, mantle plumes.

The relationship between the Tibetan Plateau and the South China Craton, and the timing and mechanism of formation of the giant Songpan–Ganzi Triassic Basin on the eastern edge of the Tibetan Plateau, have long been matters of debate (Sengor & Natal'in 1996; Chang 2000). Likewise, the role of the Permian Emeishan mantle plume in the tectonics of South China is not well understood.

The Songpan–Ganzi Basin is a huge triangular-shaped feature filled with Triassic marine flysch deposits that locally exceed 15 km in thickness (Bruguier & Malavieille 1997). It has been interpreted as a remnant ocean basin (Sengor & Natal'in 1996; Zhou & Graham 1996) and as a Permian–Triassic rift basin formed at a triple junction (Chang 2000).

The Emeishan large igneous province covers an area of more than 500,000 km^2 in the western part of the South China Craton (Zhou *et al.* 2002*a*). The geochemistry of the Emeishan continental flood basalts and their short eruption period of less than 1 Ma in the Late Permian are consistent with mantle plume volcanism (Chung & Jahn 1995; Song *et al.* 2001; Thompson *et al.* 2001; Ali *et al.* 2002; Zhou *et al.* 2002*a*). Similar metabasalts have been recognized in the Songpan–Ganzi and Yidun terranes on the eastern margin of the Tibetan Plateau (BGMS 1991; Song *et al.* 2003) (Fig. 1), but their relationship to the Emeishan continental flood basalts, 100–300 km to the east, has not been established. If these lavas are part of the Emeishan large igneous province, they place tight time constraints on rifting of the South China Craton and the formation of the Songpan–Ganzi ocean basin. Correlation of the metabasalts with the Emeishan lavas would also indicate that a huge volume of magma was erupted just prior to break-up of the western margin of the craton. The temporal and geographical coincidence of these two events implies that the Emeishan mantle plume was responsible for the break-up of the South China Craton and the formation of the Palaeo-Tethyan Songpan–Ganzi ocean basin.

The purpose of this paper is to test our proposed correlation of the Upper Permian metabasalts in the Songpan–Ganzi and Yidun terranes with the Emeishan basalts on the western South China Craton, and to investigate the role of the Emeishan plume in the tectonic evolution of the region.

Geological background

The eastern margin of the Tibetan Plateau is a complex geological zone about 200 km wide, composed of the Songpan–Ganzi and Yidun terranes. Together, these two terranes make up a giant triangular block, bounded on the north by the Kunlun–Animaqing suture from the Kunlun orogenic belt (Mattauer *et al.* 1992; Yang *et al.* 1996), on the east by the Longmenshan thrust belt from the South China Block (Burchfiel *et al.* 1995; Bruguier & Malavieille 1997), and on the west and SW by the Jinsha suture from the Qiangtang Terrane (Fig. 1).

The Songpan–Ganzi Terrane, with an area of more than 200 000 km^2, is characterized by a thick, strongly folded Triassic flysch sequence. This was derived from the Dabie–Sulu orogenic belt, to the NE, and deposited in the Songpan–Ganzi ocean basin (Yin & Nie 1993; Yin & Harrison 2000). In contrast, the NNW-trending Yidun Terrane contains mostly Lower Triassic clastic rocks and Middle–Upper Triassic calc-alkaline volcanic rocks produced by westward subduction of the Songpan–Ganzi ocean lithosphere (Fig. 1) (Hou *et al.* 2001). The Ganzi–Litang suture, which separates these two terranes, extends from west of Ganzi on the north through Litang to Muli on the south, a distance of over 1000 km (Fig. 1). Ophiolitic mélange, composed of serpentinite, gabbro, pillow basalt and chert, occurs as tectonic blocks in the Upper Triassic sedimentary rocks along this suture. The ophiolitic material was derived from the Songpan–Ganzi ocean basin (Mo *et al.* 1993; Zhong 1998).

Neoproterozoic granitic gneisses and metavolcanic rocks in the southeastern margin of the Songpan–Ganzi Terrane and the southern part of the Yidun Terrane are petrologically and geochemically comparable with Neoproterozoic basement complexes in the western margin of the South China Craton (Zhou

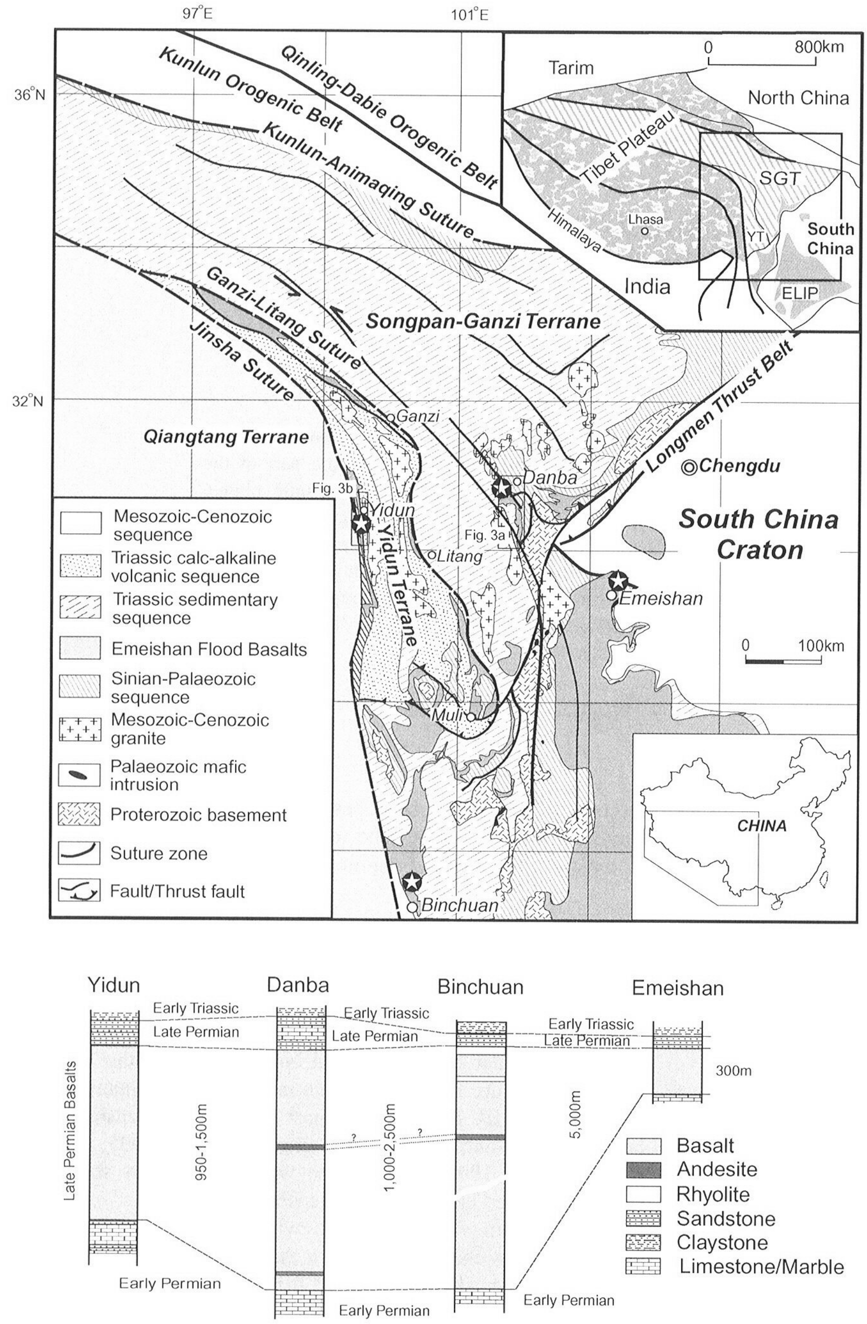

Fig. 1. Regional geological map of the Songpan–Ganzi and Yidun terranes, modified from the regional geological maps of Sichuan, Yunnan and Qinghai Provinces, China. SGT, Songpan–Ganzi Terrane; YT, Yidun Terrane; ELIP, Emeishan large igneous province. The Emeishan basalt column of Bichuan is modified after Huang *et al.* (1986), and the column at Emeishan is after Zhou *et al.* (2002*a*). Stars represent the locations of the columns.

et al. 2002*b*). These basement complexes are believed to have been formed in an arc setting above a subduction zone beneath the South China Craton at *c.* 760–860 Ma (Fig. 2) (Roger & Calassou 1997; Zhou *et al.* 2002*b*).

Along the southeastern margin of the Songpan–Ganzi Terrane and in the southern Yidun Terrane, the Neoproterozoic rocks are unconformably overlain by thick Sinian–Lower Permian continental margin shallow- to deep-marine clastic and carbonate sedimentary rocks with a few volcanic intercalations (BGMS 1991; Chang 2000) (Fig. 2). These strata are lithologically similar to Sinian–Lower Permian shallow-marine clastic sedimentary rocks and carbonates of the western part of the South China Craton (Fig. 2) (BGMS 1991). In addition, identical Ordovician to Lower Permian fossils occur in the sedimentary rocks of the three regions (Fig. 2) (BGMS 1991). Correlation of similar sedimentary sequences with the same fossils in these three tectonic blocks (BGMS 1991; Chang 2000; Yin & Harrison 2000) (Fig. 1) indicates that they were contiguous at least until Late Permian time.

Stratigraphy of the Upper Permian basalts

In their type locality at Emeishan Mountain, the Emeishan continental flood basalts lie between Lower Permian limestone and Upper Permian sandstone and mudstone. A thin, weathered zone at the base of the Emeishan continental flood basalts implies uplift and exposure of the limestone before eruption of the basalts. The Upper Permian sedimentary sequence on top of

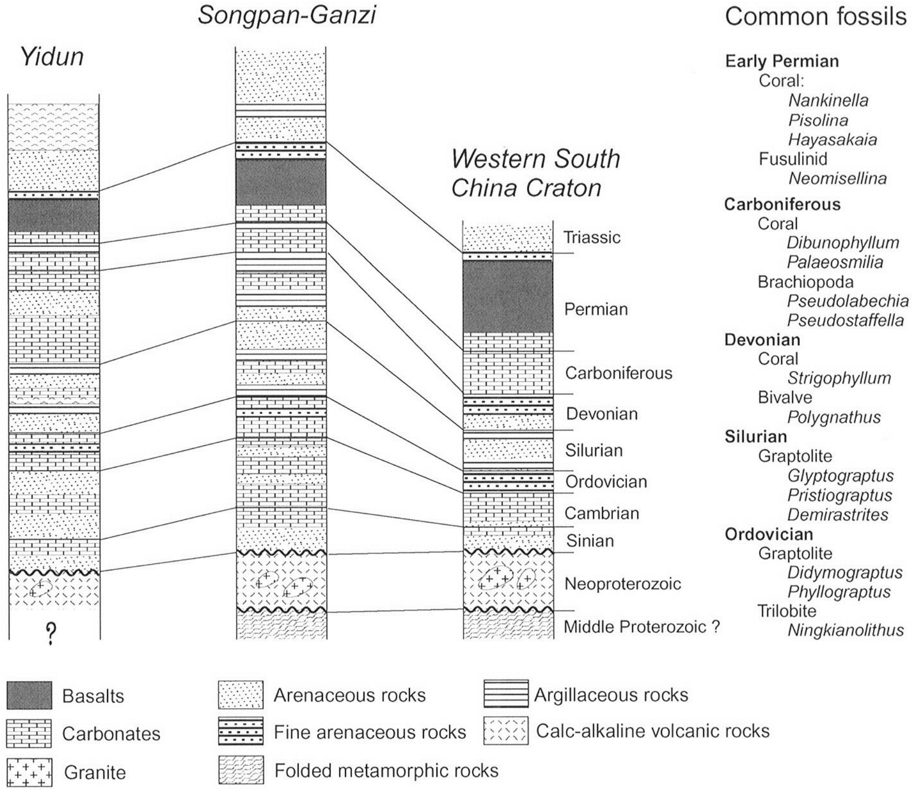

Fig. 2. Stratigraphic correlation of Proterozoic, Palaeozoic and Triassic rocks of the Songpan–Ganzi and Yidun terranes with those of the western margin of the South China Craton. Neoproterozoic calc-alkaline volcanic rocks are unconformably overlain by Sinian to Lower Permian shallow- to deep-marine clastic rocks and carbonates in the three tectonic blocks. The Ordovician to Lower Permian fossils listed in the figure are common to all three blocks (BGMS 1991).

the Emeishan continental flood basalts is, in turn, unconformably overlain by Triassic clastic rocks (Fig. 1). At Emeishan Mountain, the lavas consist dominantly of aphyric and plagioclase-phyric basalt with columnar jointing.

As shown in Figs 1 and 3a, Upper Permian metabasalts are exposed along thrust faults and around tectonic domes along the southeastern margin of the Songpan–Ganzi Terrane. In the Danba area, about 1500–2500 m of massive metabasalts disconformably overlie Lower Permian marble, which is equivalent to the Lower Permian limestone of the South China Craton, and are overlain by Uppermost Permian metasandstone, which in turn is conformably overlain by Triassic metasedimentary rocks.

In the Yidun Terrane, Upper Permian metabasalts are well exposed along major NNW-trending faults. In the western part of the terrane, a sequence of massive flows, several hundred metres to 1500 m thick, occurs in the Yidun area (Figs 1 and 3b). These basalts disconformably overlie Lower Permian marble containing fossil assemblages similar to those found in the Lower Permian limestone of the South China Craton (BGMS 1991), and are overlain by Upper Permian marble and slate (Fig. 2). The Upper Permian rocks are, in turn, overlain by Lower Triassic clastic rocks.

Correlation of the sedimentary rocks above and below the metabasalts in the Songpan–Ganzi and Yidun terranes with those in the South China Craton demonstrates that the basalts in these three areas formed at the same time, strongly suggesting that they are all part of the Emeishan large igneous province.

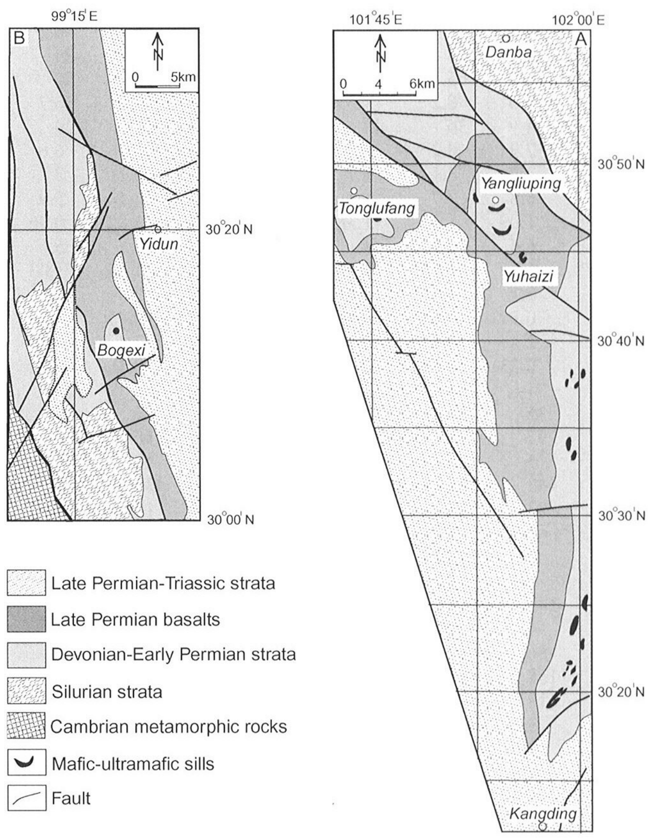

Fig. 3. (**a**) Distribution of Upper Permian basalts in the Danba area. (**b**) Distribution of Upper Permian basalts in the Yidun area.

Analytical techniques

Major oxides were determined using XRF spectrometry on fused glass discs at the University of Hong Kong. Sc, Ni and Cu were determined by

XRF on pressed powder pellets. Other trace elements, including REE, were analysed by inductively coupled plasma mass spectrometry (ICP-MS) on a VG Elemental PQ Excell system at the University of Hong Kong. We used standard additions, pure elemental standards for external calibration, and BHVO-1 as a reference material. Accuracy and precision of the XRF analyses are estimated to be ±2% for major oxides present in concentrations greater than 0.5 wt% and ±5% for trace elements. Accuracy and precision of the ICP-MS analyses are better than ±5% (Zhou *et al.* 2000).

Sm–Nd isotopic analyses were performed on a VG-354 mass spectrometer at the Institute of Geology and Geophysics, Chinese Academy of Sciences, Beijing. The mass fractionation corrections for Nd isotopic ratios were based on $^{146}Nd/^{144}Nd = 0.7219$. Detailed sample preparation and analytical procedures have been given by Zhang *et al.* (2001).

Geochemistry of the basalts

The Upper Permian metabasalts of the Songpan–Ganzi and Yidun terranes were metamorphosed under greenschist-facies conditions during Mesozoic–Cenozoic tectonometamorphic events (Huang *et al.* 2003), but this does not seem to have significantly modified their major oxide compositions. MgO

Table 1. *Contents of major oxides (wt%) and trace element abundances (ppm) of the Upper Permian metabasalts and gabbro in the Songpan–Ganzi and Yidun terranes*

	Tonglufang cross-section, Danba, Songpan–Ganzi Terrane															
	Basalt							Andesite		Basalt						
	T-3	T-4	T-5	T-6	T-8	T-9	T-10	T-12	T-13	T-14	T-15	T-16	T-18	T-20	T-21	T-25
SiO_2	47	43.7	40.7	46.4	49	49.8	49.1	57.8	59.2	49.4	46.6	45.9	49.3	48.7	46.9	49
TiO_2	3.2	3.4	4.4	3.3	2.3	2.3	2.3	1.7	1.8	2.4	1.8	1.8	3.7	2.3	2.6	2
Al_2O_3	14.1	14.4	14.4	13.7	15.7	15.1	14.4	15.3	14.4	14.9	13.8	14.4	13.7	13.8	15.9	11.6
Fe_2O_3	15	16.8	19.3	15.6	12	12.5	13.3	11.9	9.3	12.5	14.8	15.5	13.7	13.8	13.7	13.2
MnO	0.2	0.2	0.3	0.3	0.2	0.2	0.2	0.1	0.1	0.2	0.2	0.2	0.2	0.2	0.2	0.2
MgO	4.8	6.1	7.2	5.8	4.9	4.9	6	3.3	2.4	6	5.9	5.9	4.8	6.3	5.4	6.3
CaO	8.7	9.9	8.4	9.9	10.1	10.4	9.4	2.3	3.6	8.7	10.9	10.5	8.7	11.7	10.8	13.2
Na_2O	4.1	2.5	0.5	3.4	3.4	3	2.7	2.3	2.7	3.5	2.8	2.9	3.6	2.6	2.7	1.8
K_2O	0.3	0.5	2.7	0.7	1	0.7	1.3	2.3	2.4	0.5	1	1.2	1.1	0.4	0.4	0.4
P_2O_5	0.6	0.5	0.6	0.5	0.3	0.3	0.3	0.1	0.2	0.3	0.2	0.2	0.4	0.2	0.3	0.3
LOI	1.3	1.7	1.3	0.3	0.8	1.1	2.6	2.9	2.7	1.7	1.8	1.4	0.3	0.6	0.8	2.2
Total	99.4	99.9	99.8	99.8	99.5	100.2	101.4	99.9	98.9	100.1	99.8	99.9	99.4	100.5	99.6	100.1
Mg no.	41.5	45	45.5	45.1	47.5	46.7	50.2	38.3	36.7	51.6	47	45.8	43.7	50.3	46.9	51.4
La	26	28	32	26	29	30	24	89	54	32	17	17	44	24	26	21
Ce	61	65	76	60	66	67	55	175	114	72	36	37	102	53	60	47
Pr	7.6	8.2	9.5	7.7	8.3	8.3	6.7	18	13	8.8	4.2	4.5	12.6	6.5	7.5	6
Nd	34	36	42	34	35	35	29	70	50	37	18	19	52	28	33	26
Sm	7.9	8.2	9.5	7.5	7.6	7.5	6.6	13	10	7.8	4.1	4.8	11.4	6.7	7.2	5.7
Eu	2.7	3.1	3.7	2.7	2.6	2.2	2	3	2	2.4	1.3	1.5	3.1	2.1	2.3	1.7
Gd	6.8	7.7	8.5	7	6.3	6.5	5.9	12	9	7.1	4.5	4.7	9.6	6.4	6.4	5.1
Tb	1.09	1.18	1.38	1.1	0.98	1.02	0.96	1.86	1.46	1.05	0.76	0.84	1.41	1	1.02	0.81
Dy	6.4	6.9	8	6.3	5.7	6	5.6	11	8.4	6	5	5.5	7.8	6	5.8	4.7
Ho	1.16	1.22	1.46	1.13	1.05	1.08	1.03	2.12	1.6	1.08	1	1.11	1.42	1.14	1.06	0.86
Er	3.1	3.3	3.8	3	2.7	3	2.8	6.3	4.47	3	2.9	3.2	3.7	3.1	2.8	2.3
Tm	0.39	0.44	0.53	0.41	0.37	0.41	0.37	0.91	0.61	0.4	0.39	0.46	0.49	0.41	0.37	0.29
Yb	2.4	2.7	3.2	2.5	2.3	2.4	2.2	5.57	3.94	2.6	2.6	2.9	2.9	2.6	2.2	1.8
Lu	0.33	0.39	0.44	0.35	0.33	0.36	0.32	0.75	0.55	0.34	0.4	0.43	0.39	0.34	0.28	0.27
Y	31	34	39	32	29	31	29	60	45	29	27	32	40	32	30	25
Sc	35	36	43	33	33	32	31	23	26	33	41	46	33	32	30	33
Ba	97	274	1015	207	336	240	437	251	238	134	221	304	278	102	99	102
Rb	5	7	65	11	23	14	26	75	80	15	23	32	32	7	5	7
Sr	443	504	677	343	525	431	632	140	142	311	225	252	366	469	574	406
Nb	23	26	31	22	18	19	22	65	67	18	20	22	38	19	18	15
Ta	1.4	1.5	1.8	1.3	1.1	1	1.3	3.9	3.4	1.1	1.1	1.2	2.2	1	0.9	0.8
Th	3	3.1	3.9	2.8	3.8	4.2	3.3	13.9	9.5	4.4	2.9	2.9	8	3.4	2.7	2.4
U	1.4	1	1	0.8	1.1	1.1	0.9	2.1	3.6	0.9	0.7	0.6	1.9	1.1	0.7	0.6
Zr	149	153	180	126	199	183	157	456	398	208	97	97	266	130	108	132
Hf	4	3.8	4.7	3.3	5.1	4.4	4	11.7	9.3	5.4	2.6	2.5	6.4	3.4	2.7	3.2
Ni	86	82	97	95	60	57	90	80	133	75	83	54	63	99	81	93
Cu	158	116	349	148	149	118	150	99	99	158	224	214	188	112	82	125
Ti/Y	619	599	678	620	476	448	476	168	244	492	392	326	555	419	512	476
La/Sm	3.4	3.4	3.4	3.5	3.9	4.1	3.7	6.7	5.3	4.1	4.2	3.6	3.9	3.6	3.6	3.6
Gd/Yb	2.9	2.9	2.6	2.8	2.8	2.7	2.7	2.1	2.3	2.7	1.7	1.6	3.3	2.5	2.9	2.8
Ba/Nb	4.3	10.51	33.12	9.39	18.3	12.86	19.75	3.86	3.58	7.29	11.14	13.66	7.41	5.27	5.37	6.67
Zr/Nb	6.6	5.86	5.86	5.72	10.86	9.8	7.1	7.02	5.97	11.31	4.89	4.34	7.07	6.76	5.9	8.67
La/Nb	1.17	1.06	1.04	1.17	1.59	1.63	1.1	1.38	0.81	1.74	0.87	0.78	1.18	1.24	1.42	1.36
Th/La	0.11	0.11	0.12	0.11	0.13	0.14	0.13	0.16	0.18	0.14	0.17	0.17	0.18	0.14	0.1	0.11

Fe_2O_3 represents total Fe. LOI, loss on ignition.

contents range from 4.8 to 7.2 wt%, SiO_2 from 39.2 to 49.8 wt%, and TiO_2 from 1.6 to 4.2 wt% (Table 1). Mg numbers, where Mgnumber $= 100Mg^{2+}/(Fe^{2+} + Mg^{2+})$ and Fe^{2+} is 89% total iron, range from 40.1 to 54.1. On a SiO_2 v. $(Na_2O + K_2O)$ diagram (Le Maitre *et al.* 1989) the lavas from the Songpan–Ganzi Terrane plot chiefly in the basalt field on both sides of the alkali–tholeiite boundary as defined by Irvine & Baragar (1971) (Fig. 4). Those from the Yidun Terrane mostly lie in the field of alkali basalts. All but three of the analysed samples plot in the Emeishan continental flood basalts field as defined by Song *et al.* (2001) and Xu *et al.* (2001) (Fig. 4). On plots of Mg number v. TiO_2, Fe_2O_3, Al_2O_3 and $Na_2O + K_2O$ the lavas also clearly lie within the field of the Emeishan continental flood basalts of the South China Craton (Fig. 5).

Consistent with the major oxide geochemistry, chondrite-normalized REE patterns of the Upper Permian metabasalts of the Songpan–Ganzi and Yidun terranes are virtually identical to those of the type Emeishan basalts. All of the analysed samples are characterized by marked light REE enrichment (LREE; La/Sm = 3.4–4.3) and heavy REE depletion (HREE; Gd/Yb = 2.4–3.0) (Table 1, Fig. 6a and b). Primitive mantle-normalized trace element patterns show that all the basalts are

Bogexi cross-section, Yidun, Yidun Terrane													
Basalt													
B02-1	B02-2	B02-3	B02-4	B02-5	B02-13	B02-14	B02-15	B02-16	B02-17	B02-18	B02-19	B02-20	B02-21
45.4	45.6	48	46.9	48	44.5	46.6	46.8	46.6	47.8	45.8	46.3	46	46.9
3.3	3.4	2.7	2.5	2.5	3.8	2.9	2.8	3.4	3.3	3.2	2.8	2.6	3.5
13.5	13.5	14	14	13.7	13.8	13.2	13.7	13.3	12.8	13.3	13.7	12.8	13.3
15.7	15.6	13.2	12.5	12.9	15.2	15	14.3	15.2	15.4	14.9	14.1	13.4	15.2
0.2	0.2	0.2	0.2	0.2	0.2	0.2	0.2	0.3	0.3	0.2	0.2	0.2	0.2
5.4	5.3	5.7	6.6	6.3	6.3	5	5.6	5.1	4.6	6.7	5.4	4.8	4.9
9.4	9.3	8.9	10.4	9.7	7.1	8.7	6.8	10	6.4	5.9	8.2	10	6.3
3.1	3.1	3	2.6	2.9	2.8	3.1	3.6	2.5	3.8	3.4	3.5	2.9	3.6
1	0.9	1.3	0.9	0.8	1.2	1	1.2	1.1	0.5	0.9	1.4	1.1	0.7
0.6	0.6	0.4	0.4	0.3	0.8	0.6	0.6	0.6	0.7	0.6	0.6	0.5	0.7
1.9	2	2.2	2.3	2	3.7	3	3.9	2.6	3.8	3.6	3	4.7	3.5
99.4	99.5	99.7	99.3	99.3	99.5	99.5	99.5	100.7	99.3	98.4	99.3	99.1	98.9
43.6	42.9	49.1	54.1	52.4	48.1	42.8	46.6	42.9	40.1	50	46	44.5	42
30	33	28	23	24	31	38.46	36	34	34	32	36	31	37
68	74	61	53	54	70	85.38	81	76	75	72	77	70	83
9	9.6	7.8	6.9	7	9.2	11.11	10.7	9.7	9.8	9.3	9.9	9.2	10.9
39	42	33	30	30	40	47.61	46	42	42	40	42	39	47
7.9	8.4	7.2	6.5	6.5	8.2	9.47	9.8	8.8	8.9	8.6	8.2	8.4	10
3.1	3.2	2.5	2.2	2.2	3.4	3.37	3.9	3.1	2.8	3.1	2.8	3.3	3.2
6.8	7.2	6.7	6.1	6	7.2	8.17	9.1	8.2	8.3	7.9	7.2	7.8	9.1
1.07	1.16	1.13	1.04	1.02	1.12	1.3	1.52	1.38	1.37	1.33	1.15	1.31	1.55
5.7	6.1	6.4	5.8	5.7	6.1	6.87	8.4	7.7	7.5	7.4	6.1	7.2	8.5
1.11	1.16	1.24	1.13	1.14	1.15	1.32	1.62	1.5	1.47	1.43	1.18	1.41	1.64
3	3.1	3.4	3	3	3.1	3.51	4.3	3.9	3.9	3.9	3.1	3.8	4.4
0.35	0.38	0.44	0.39	0.4	0.38	0.43	0.55	0.5	0.49	0.49	0.38	0.48	0.56
2.3	2.5	2.8	2.6	2.5	2.4	2.81	3.6	3.3	3.3	3.2	2.5	3.1	3.6
0.33	0.36	0.42	0.37	0.37	0.36	0.41	0.53	0.48	0.47	0.47	0.36	0.47	0.53
27	28	31	28	28	28	32.71	40	36	37	36	29	36	41
25	25	28	29	28	31	25.3	31	26	25	28	24	26	29
543	482	279	241	254	414	582	422	415	1155	427	590	649	311
27	18	25	26	16	32	32.09	23	39	18	19	26	27	17
495	560	580	270	351	346	879	206	950	262	147	355	540	433
24	26	23	20	21	25	26.66	29	28	28	26	26	26	30
1.6	1.7	1.5	1.3	1.4	1.7	1.7	1.9	1.9	1.8	1.7	1.6	1.7	2
3.2	3.4	3.8	3.1	3.3	3.1	3.8	4.7	4.2	4.2	4	3.5	4.1	4.7
0.8	0.9	1	0.8	0.9	0.8	0.95	1.2	1.1	1.1	1.1	0.8	1.2	1.3
166	177	189	177	184	163	178	226	213	212	206	166	205	233
4.3	4.5	4.8	4.5	4.7	4.2	4.41	5.8	5.5	5.4	5.2	4.1	5.2	6.2
50	45	86	118	106	88	42.2	53	49	43	57	47	49	47
73	78	88	144	138	135	104.3	66	77	47	71	70	72	53
751	720	522	546	531	812	540	418	564	535	529	585	434	515
3.8	3.9	3.8	3.6	3.7	3.8	4.1	3.7	3.8	3.7	3.7	4.3	3.7	3.7
3	2.9	2.4	2.4	2.4	2.9	2.9	2.6	2.5	2.5	2.5	2.9	2.5	2.5
22.39	18.59	12.08	11.82	12.01	16.86	21.83	14.33	14.94	41.63	16.34	23.03	24.56	10.2
6.83	6.85	8.17	8.68	8.67	6.64	6.64	7.66	7.66	7.64	7.89	6.49	7.77	7.65
1.25	1.27	1.2	1.15	1.14	1.27	1.27	1.24	1.21	1.21	1.23	1.39	1.19	1.21
0.1	0.1	0.14	0.13	0.14	0.1	0.1	0.13	0.12	0.12	0.12	0.1	0.13	0.13

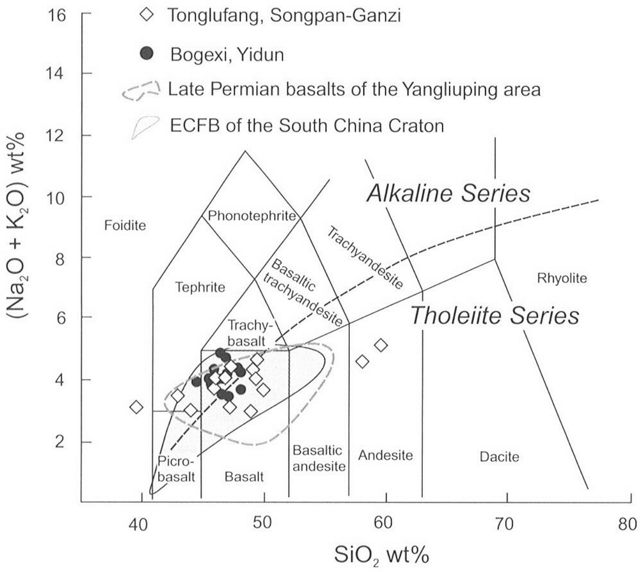

Fig. 4. Chemical classification and nomenclature of volcanic rocks using the total alkalis v. silica (TAS) diagram of Le Maitre *et al.* (1989). The subdivision of alkaline and tholeiitic series is after Irvine & Baragar (1971). Data for the Emeishan continental flood basalts are after Song *et al.* (2001) and Xu *et al.* (2001). ECFB, Emeishan continental flood basalts.

enriched in both high field strength elements and large ion lithophile elements (Fig. 6c and d) (Song *et al.* 2001; Xu *et al.* 2001).

The geochemical data also suggest that the parental melts of the Yidun and Songpan–Ganzi basalts were predominantly derived from the Emeishan plume. The basalts have variable trace element ratios, such as Zr/Nb (4.34–11.31), La/Nb (0.73–1.74), Ba/Nb (4.30–41.63) and Th/La (0.10–0.19) (Table 1), that are virtually identical to those of the Emeishan continental flood basalts (Song *et al.* 2001). In a Ce/Nb v. Th/Nb diagram, the Upper Permian metabasalts clearly lie in the field of the Emeishan continental flood basalts and extend from ocean-island basalt (OIB) to the field of intra-oceanic arc basalts (Fig. 7). This trend can be interpreted in terms of interaction between primitive magmas and the subcontinental lithosphere (Davies *et al.* 1989; Hofmann 1997; Green & Falloon 1998; Hauff *et al.* 2000).

In addition, the metabasalts and gabbros of the Songpan–Ganzi and Yidun terranes have similar $\varepsilon_{Nd(t)}$ values (−0.3 to 4.8) (Table 2), which plot within the field defined by the Emeishan continental flood basalts (−6 to +6) (Fig. 8) (Xu *et al.* 2001).

The similar geochemical characteristics outlined above indicate that the parental melts of the basalts of the Songpan–Ganzi and Yidun terranes were derived from the same source regions as the Emeishan continental flood basalts. Song *et al.* (2001) proposed that the primitive magmas of the Emeishan continental flood basalts were produced by partial melting of a rising mantle plume that reacted with the lithospheric mantle, which had been previously modified and enriched by pelagic sediments during Neoproterozoic subduction. The depletion of HREE and the large Gd/Yb ratios in these rocks are interpreted to reflect partial melting of garnet lherzolite at depths of 60–70 km or more.

In summary, all of the geochemical characteristics described above support the correlation of the Upper Permian metabasalts in the Songpan–Ganzi and Yidun terranes with those in the type location of the Emeishan flood basalts and indicate that they were derived from the same melt source regions.

Tectonic implications

One of the most important regional geological problems in eastern Tibet is the origin of the Songpan–Ganzi basin and the Triassic flysch with which it is filled. Some workers have suggested that the flysch detritus was derived from the Sulu–Dabie orogenic belt and deposited in a remnant ocean basin (Yin & Nie 1993; Zhou & Graham 1996; Ingersoll *et al.* 1995).

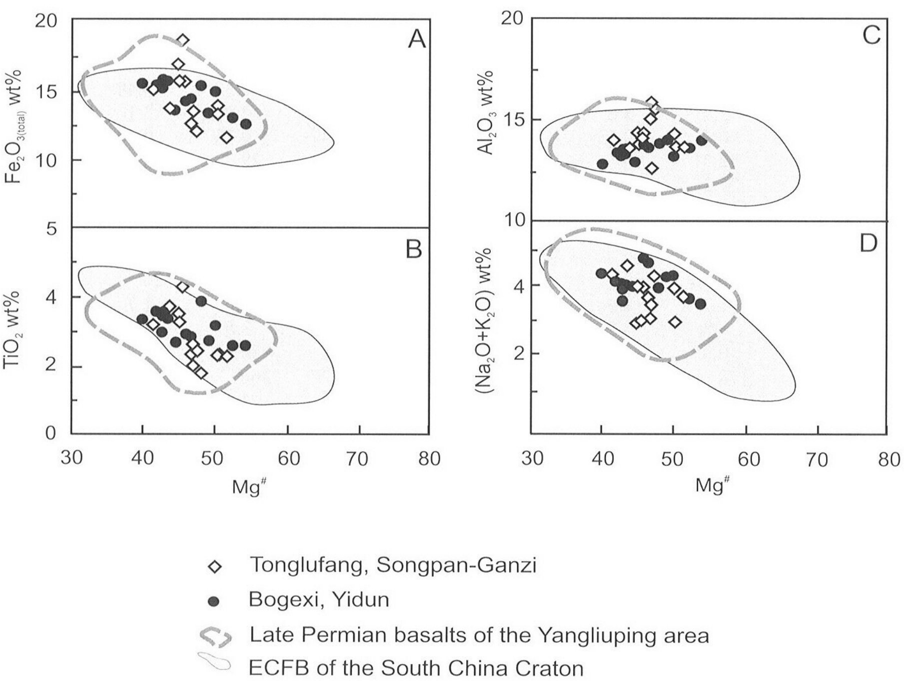

Fig. 5. Correlation between Mg number and oxides. The compositions of the Emeishan continental flood basalts (ECFB) are represented by the shaded areas. The fields circled by dashed lines represent the compositions of the basalts in the Danba area (unpublished data). Data for the Emeishan continental flood basalts are after Song *et al.* (2001) and Xu *et al.* (2001).

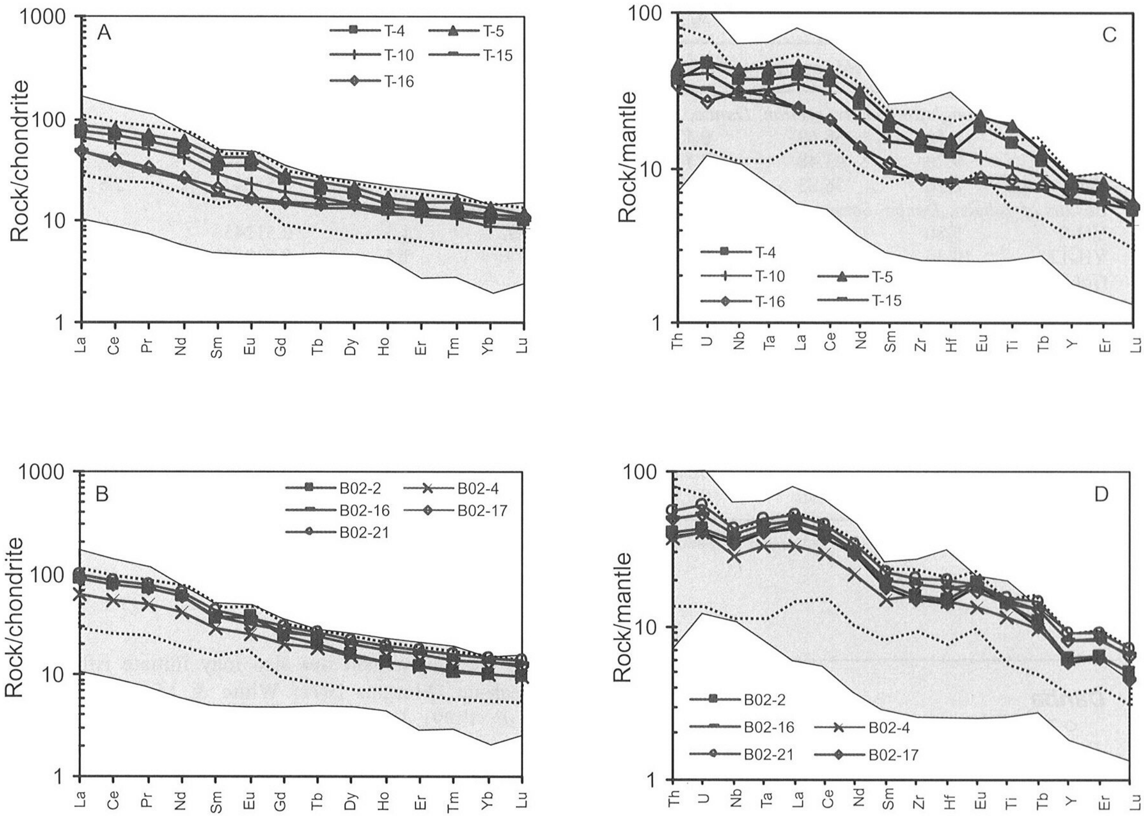

Fig. 6. (**a**, **b**) Selected chondrite-normalized REE patterns of Upper Permian basalts in the Songpan–Ganzi and Yidun terranes: (**a**) Tonglufang section, Danba; (**b**) Bogexi section, Yidun. Normalization values are after Taylor & McLennan (1985). (**c**, **d**) Selected primitive mantle-normalized trace-element patterns of Upper Permian basalts in the Songpan–Ganzi and Yidun terranes: (**c**) Tonglufang section, Danba; (**d**) Bogexi section, Yidun. Primitive mantle values are after Hofmann (1988). The shaded areas show the limits of the Emeishan continental flood basalts, data after Song *et al.* (2001) and Xu *et al.* (2001). The fields circled by dashed lines mark the limits of the basalts in the Danba area (unpublished data).

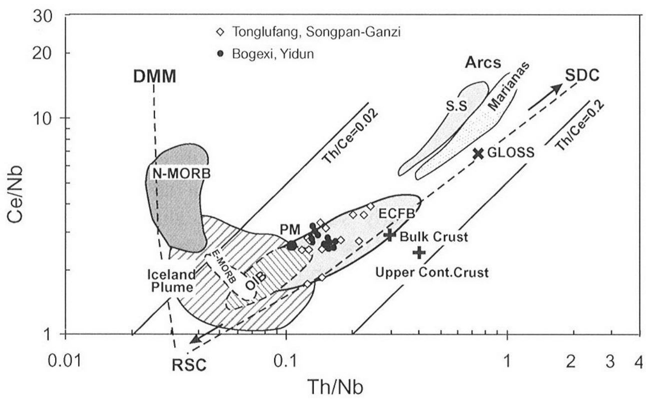

Fig. 7. Diagram of Ce/Nb v. Th/Nb. The Upper Permian metabasalts plot within the field of the Emeishan continental flood basalts. DMM, depleted mantle; SDC, recycled subduction-derived component; S.S, subducting sediments in arcs; RSC, recycled residual slab composition; OIB, ocean-island basalt; N-MORB, normal mid-ocean ridge basalt; E-MORB, enriched MORB; PM, primitive mantle. The compositions of upper continental crust and bulk continental crust are modified fromSaunders *et al.* (1988, 1991). Data for the Iceland plume are from Hemond *et al.* (1993). Fields for arcs are from Saunders *et al.* (1991). Global subducting sediment composition (GLOSS) is from Plank & Langmuir (1998).

However, the remnant ocean basin model poses several problems. First, similar Neoproterozoic rocks and Sinian–Palaeozoic sedimentary rocks occur on the eastern margins of the Songpan–Ganzi Yidun terranes and the western margin of the South China Craton (Fig. 3). Second, this model does not account for the presence of the Emeishan continental flood basalts in the Songpan–Ganzi and Yidun terranes (Fig. 1). Finally, the geochemistry of early Mesozoic plutons within the Songpan–Ganzi Terrane suggests that they were derived from underlying continental crust (Burchfiel *et al.* 1995). Chang (2000) proposed that a triple junction developed in the Songpan–Ganzi Terrane during the Permian and detritus from the Dabie–Sulu belt and adjacent areas filled the new oceanic basin. However, Chang's model does not address the cause of rifting in the Late Permian.

Correlation of the Neoproterozoic and Palaeozoic rocks in the Songpan–Ganzi and Yidun terranes along the eastern edge of the Tibet Plateau with those of the South China Craton indicates that these regions were contiguous until the Late Permian. Identification of Emeishan basalts on both sides of the Ganzi–Litang suture indicates that the Songpan–Ganzi ocean basin opened in the latest Permian by break-up of the South China Craton. The spatial and temporal relationships between the break-up and the development of the Emeishan basalts suggest that the initial rifting and development of the ocean basin at the triple junction were a response to the plume activity. Extensive uplift of the lithosphere along the western margin of the South China Craton,

Table 2. *Sm–Nd isotopic data for the Upper Permian metabasalts of the Songpan–Ganzi and Yidun terranes*

Sample	Sm (ppm)	Nd (ppm)	$^{147}Sm/^{144}Nd$	$^{143}Nd/^{144}Nd$	$\pm 2\sigma$ ($\times 10^5$)	$^{143}Nd/^{144}Nd_t$	εNd(260 Ma)
Basalts of the Tonglufang cross- section, Danba, Songpan–Ganzi Terrane							
T-4	8.68	38.69	0.136	0.512621	1.1	0.51239	1.7
T-5	9.70	43.48	0.135	0.512671	1.0	0.51244	2.7
T-6	8.20	36.83	0.135	0.512661	1.1	0.51243	2.5
Basalts of Yuhaizi, Danba, Songpan–Ganzi Terrane							
YH-9	7.80	34.95	0.135	0.512681	1.5	0.51245	2.9
YH-12	10.36	47.29	0.133	0.512773	1.5	0.51255	4.8
Gabbro of the Yuhaizi intrusion, Danba, SGT							
YH-31	7.82	33.58	0.141	0.512699	0.8	0.51246	3.1
YH-34	3.94	15.05	0.158	0.5127	1.0	0.51243	2.5
YH-36	3.39	12.88	0.159	0.512751	1.4	0.51248	3.5
Basalts of the Bogexi cross-section, Yidun, Yidun Terrane							
B02-13	8.26	40.28	0.124	0.51254	1.4	0.51233	0.5
B02-15	10.19	47.31	0.130	0.512508	1.0	0.51229	−0.3
B02-16	9.61	43.28	0.134	0.512534	1.1	0.51231	0.04
B02-18	8.60	39.16	0.133	0.512561	0.9	0.51234	0.6
B02-20	8.57	38.56	0.134	0.512584	1.1	0.51236	1.0

$^{143}Nd/^{144}Nd$ normalized to $^{146}Nd/^{144}Nd = 0.7219$. Estimated overall error is ± 0.000020.

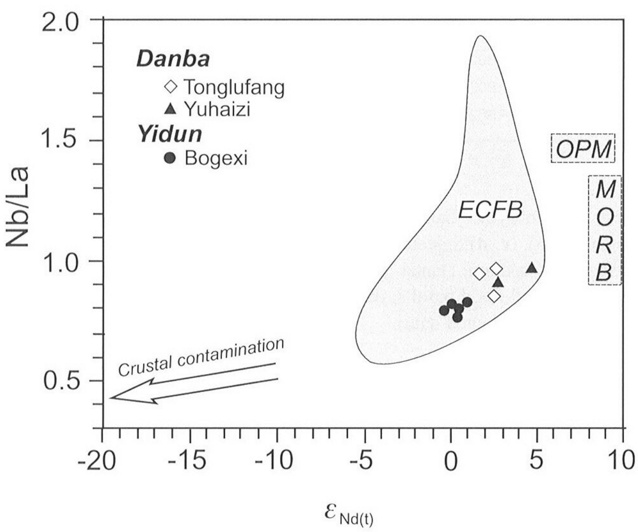

Fig. 8. Correlation between Nb/La and $\varepsilon_{Nd(t)}$ of the Upper Permian metabasalts from Danba and Yidun. The field of the Emeishan continental flood basalts (ECFB) is from Xu *et al.* (2001). OPM, average oceanic plume magma (Gibson *et al.* 1996). The tendency of crustal contamination is modified from Weaver & Tarney (1984), Taylor & McLennan (1985) and Wilson (1989).

prior to eruption of the basalts, is indicated by the disconformity between the Lower Permian limestone or marble and the Emeishan continental flood basalts. As the mantle plume welled upward during lithospheric thinning and extension, rapid decompressional melting produced huge volumes of magma. Continued rifting is believed to have led to formation of the Songpan–Ganzi ocean basin, which was later filled with huge quantities of clastic sediment. Westward subduction of the Songpan–Ganzi oceanic lithosphere in the Late Triassic caused extensive calc-alkaline volcanism and intrusion along the Yidun Terrane in the Late Triassic (Hou *et al.* 2001).

Other workers have previously proposed that the sublithospheric impact of mantle plumes not only causes extensive basaltic magmatism but also may initiate rifting and continent break-up (Morgan 1971; White & McKenzie 1995; Courtillot *et al.* 1999). For example, fragmentation of Pangaea during the Mesozoic and Cenozoic has been linked to mantle plume impact (Dalziel *et al.* 2000), and Courtillot *et al.* (1999) suggested that a huge extensional basin, which opened in the latest Permian or earliest Triassic at the western margin of the Siberian Traps, may have been triggered by the mantle plume from which the parental melts of the basalts were derived. The relationship between activity of the Emeishan mantle plume and opening of the Songpan–Ganzi ocean basin and break-up of the South China Craton provides another example.

Conclusions

The Upper Permian lavas in the Songpan–Ganzi and Yidun terranes represent distal members of the Emeishan continental flood basalts produced by the Emeishan mantle plume. Uplift and extension of the lithosphere by the mantle plume in the Late Permian caused the formation of a triple junction in the region, break-up of the South China Craton and opening of the Songpan–Ganzi ocean basin. The Emeishan continental flood basalts erupted in the early stages of uplift and rifting of the South China Craton, and are considered to be tectonically equivalent to dipping reflectors on modern ocean margins.

This study was supported by the Research Grant Council of the Hong Kong SAR, China (HKU7101/01P and HKU7056/03P) to M.-F.Z. A postgraduate studentship from the University of Hong Kong, and grants from China (NSFC Nos 40373030 and 40273025) to X.-Y.S. are acknowledged.

References

Ali, J.-R., Thompson, G.-M., Song, X.-Y. & Wang, Y.-L. 2002. Emeishan Basalts (SW China) and the 'end-Guadalupian' crisis; magnetobiostratigraphic constraints. *Journal of the Geological Society, London*, **159**, 21–29.

BGMS 1991. *Regional Geology of Sichuan Province*. Bureau of Geology and Mineral Resources of Sichuan Province. Geological Publishing House, Beijing.

Bruguier, O. & Malavieille, J.R. 1997. U–Pb dating on single detrital zircon granites from the Triassic Songpan–Ganzi flysch (Central China); provenance and tectonic correlation. *Earth and Planetary Science Letters*, **152**, 217–231.

BURCHFIEL, B.C., CHEN, Z., LIU, Y. & ROYDEN, L.H. 1995. Tectonics of the Longmen Shan and adjacent regions, central China. *International Geology Review*, **37**, 661–735.

CHANG, E.Z. 2000. Geology and tectonics of the Songpan–Ganzi fold belt, Southwestern China. *International Geology Review*, **42**, 813–831.

CHUNG, S.L. & JAHN, B.-M. 1995. Plume–lithosphere interaction in generation of the Emeishan flood basalts at the Permian–Triassic boundary. *Geology*, **23**, 889–892.

COURTILLOT, V., JAUPART, C., MANIGHETTI, P. & BESSE, J. 1999. On causal links between flood basalts and continental break-up. *Earth and Planetary Science Letters*, **166**, 177–195.

DALZIEL, I.W.D., LAWVER, L.A. & MURPHY, J.B. 2000. Plumes, orogenesis, and supercontinental fragmentation. *Earth and Planetary Sciences Letters*, **178**, 1–11.

DAVIES, G.R., NORRY, M.J., GERLACH, D.C. & CLIFF, R.A. 1989. A combined chemical and Pb–Sr–Nd isotope study of the Azores and Cape Verde hotspots: the geodynamic implications. *In:* SAUNDERS, A.D. & NORRY, M.J. (eds) *Magmatism in the Ocean Basins*. Geological Society, London, Special Publications, **42**, 231–256.

GIBSON, S.A., THOMPSON, R.N., DICKIN, A.P. & LEONARDOS, O.H. 1996. Mafic potassic magmatic key to plume–lithosphere interactions and continental flood-basalts. *Earth and Planetary Science Letters*, **141**, 325–341.

GREEN, D.H. & FALLOON, T.J. 1998. A Ringwood concept and its current expression. *In:* JACKSON, I. (ed.) *The Earthpos;s Mantle–Composition, Structure, and Evolution*. Cambridge University Press, Cambridge, 311–381.

HAUFF, F., HOERNLE, K., TILTON, G., GRAHAM, D.W. & KERR, A.C. 2000. Large volume recycling of oceanic lithosphere over short time scale: geochemical constraints from the Caribbean Large Igneous Province. *Earth and Planetary Science Letters*, **174**, 247–263.

HEMOND, C., ARNDT, N.T., LICHTENSTEIN, U., HOFMANN, A.W., OSKARSSON, N. & STEINTHORSSON, S. 1993. The heterogeneous Iceland plume: Nd–Sr–O isotope and trace element constraints. *Journal of Geophysical Research*, **98**, 15833–15850.

HOFMANN, A.W. 1988. Chemical differentiation of the Earth: the relationship between mantle, continental crust, and oceanic crust. *Earth and Planetary Science Letters*, **90**, 297–314.

HOFMANN, A.W. 1997. Mantle geochemistry: the message from oceanic volcanism. *Nature*, **385**, 219–229.

HOU, Z.Q., CHEN, W. & LU, J.R. 2001. Collision event during 177–135 Ma on the eastern margin of the Qinghai–Tibetan Plateau: evidence from $^{40}Ar/^{39}Ar$ dating for basalts on the western margin of the Yangtze platform. *Acta Geologica Sinica*, **76**(2), 194–204.

HUANG, K.N., OPDYKE, N.D., KENT, D.V., XU, G.Z. & TANG, R.L. 1986. Further paleomagnetic results from the Permian Emeishan basalts in SW China. *Kexue Tongbao*, **31**, 1195–1201 (in Chinese).

HUANG, H., MAAS, R., BUICK, I.S. & WILLIAMS, I.S. 2003. Crustal response to continental collisions between the Tibet, India, South China and North China Blocks: geochronological constraints from the Songpan–Ganze Orogenic Belt, western China. *Journal of Metamorphic Geology*, **21**, 223–240.

INGERSOLL, R.V., GRAHAM, S.A. & DICKINSON, W.R. 1995. Remnant-ocean-basins. *In:* BUSBY, C. & INGERSOLL, R.V. (eds) *Tectonics of Sedimentary Basins*. Blackwell, Oxford, 1–51.

IRVINE, T.N. & BARAGAR, W.R.A. 1971. A guide to the chemical classification of common volcanic rocks. *Canadian Journal of Earth Sciences*, **8**, 523–548.

LE MAITRE, R.W., BATEMAN, P. & DUDEK, A. ET AL. 1989. *A Classification of Igneous Rocks and Glossary of Terms*. Blackwell Scientific, London.

MATTAUER, M., MATTE, P.H. & MALAVIEILLE, J. ET AL. 1992. The Songpan–Ganzi Triassic belt of W Sichuan on eastern Tibet. *Comptes Rendus de l'Academie des Sciences, Serie 2*, **314**, 619–626.

MO, X.X., LU, F.X. & SHEN, S.Y. ET AL. 1993. *Volcanism and Mineralization in the Sanjiang Tethys*. Geological Publishing House, Beijing (in Chinese).

MORGAN, W.J. 1971. Convection plumes in the lower mantle. *Nature*, **230**, 42–43.

PLANK, T. & LANGMUIR, C.H. 1998. The chemical composition of subducting sediment and its consequences for the crust and mantle. *Chemical Geology*, **145**, 325–394.

ROGER, F. & CALASSOU, S. 1997. Géochronologie U–Pb sur zircons et géochimie (Pb, Sr, Nd) du socle de la chaîne de Songpan–Garze (China). *Geochemistry*, **324**, 819–826.

SAUNDERS, A.D., NORRY, M.J. & TARNEY, J. 1988. Origin of MORB and chemically depleted mantle reservoirs: trace element constraints. *Journal of Petrology, Special Lithosphere Issue*, 415–445.

SAUNDERS, A.D., NORRY, M.J. & TARNEY, J. 1991. Fluid influence on the trace element compositions of subduction zone magmas. *Philosophical Transactions of the Royal Society, London, Series A*, **335**, 337–392.

SENGOR, A.M.C. & NATAL'IN, B.A. 1996. Paleotectonics of Asia: fragments of a synthesis. *In:* YIN, A. & HARRISON, M. (eds) *The Tectonic Evolution of Asia*. Cambridge University Press, Cambridge, 486–640.

SONG, X.-Y., ZHOU, M.-F., HOU, Z.-Q., CAO, Z.-M., WANG, Y.-L. & LI, Y.-G. 2001. Geochemical constraints on the mantle source of the Upper Permian Emeishan continental flood basalts, Southwestern China. *International Geology Review*, **43**, 213–225.

SONG, X.-Y., ZHOU, M.-F., CAO, Z.-M., SUN, M. & WANG, Y.-L. 2003. The Ni–Cu–(PGE) magmatic sulfide deposits in the Yangliuping area within the Permian Emeishan Large Igneous Province, SW China. *Mineralium Deposita*, **38**, 831–843.

TAYLOR, S.R. & MCLENNAN, S.M. 1985. *The Continental Crust: its Composition and Evolution*. Blackwell Scientific, London.

THOMPSON, G.-M., ALI, J.-R., SONG, X.-Y. & JOLLEY, D.-W. 2001. Emeishan Basalts, SW China; reappraisal of the formation's type area stratigraphy and a discussion of its significance as a large igneous province. *Journal of the Geological Society, London*, **158**(4), 593–599.

WEAVER, B. & TARNEY, J. 1984. Empirical approach to estimating the composition of the continental crust. *Nature*, **310**, 575–577.

WHITE, R.S. & MCKENZIE, D.P. 1995. Mantle plumes and continental flood basalts. *Journal of Geophysical Research*, **100**, 17543–17585.

WILSON, M. 1989. *Igneous Petrogenesis – a Global Tectonic Approach*. Unwin Hyman, London.

XU, Y.-G., CHUNG, S.L., JAHN, B.M. & WU, G.-Y. 2001. Petrologic and geochemical constraints on the petrogenesis of Permian–Triassic Emeishan flood basalts in southwestern China. *Lithos*, **58**(3-4), 145–168.

YANG, J.-S., ROBINSON, P.T., JIANG, C.-F. & XU, Z.-Q. 1996. Ophiolites of the Kunlun Mountains, China and their tectonic implications. *Tectonophysics*, **258**, 215–231.

YIN, A. & HARRISON, T.M. 2000. Geologic evolution of the Himalayan–Tibetan orogen. *Annual Review of Earth and Planetary Sciences*, **28**, 211–280.

YIN, A. & NIE, S. 1993. An indentation model for North and South China collision and the development of the Tanlu and Honam fault system, eastern Asia. *Tectonics*, **12**, 801–813.

ZHANG, H.F., SUN, M., LU, F.X., ZHOU, X.H., ZHOU, M.-F., LIU, Y.S. & ZHANG, G.H. 2001. Geochemical significance of a garnet lherzolite from the Dahongshan kimberlite, Yangtze Craton, southern China. *Geochemistry Journal*, **35**, 315–331.

ZHONG, D.-L. 1998. *The Paleo-Tethys Orogenic Belt in the Western Yunnan and Sichuan, China*. Scientific Publishing House, Beijing.

ZHOU, D. & GRAHAM, S.A. 1996. The Songpan–Ganzi complex of the western Qinling Shan as a Triassic remnant ocean basin. *In:* YIN, A. & HARRISON, T.M. (eds) *The Tectonic Evolution of Asia*. Cambridge University Press, Cambridge, 281–299.

ZHOU, M.-F., ZHAO, T.-P., MALPAS, J. & SUN, M. 2000. Crustal-contaminated komatiitic basalts in southern China: products of Proterozoic mantle plume underneath the Yangtze Block. *Precambrian Research*, **103**, 175–189.

ZHOU, M.-F., MALPAS, J. & SONG, X.-Y. ET AL. 2002a. A temporal link between the Emeishan large igneous province (SW China) and the end-Guadalupian mass extinction. *Earth and Planetary Science Letters*, **196**, 113–122.

ZHOU, M.-F., YAN, D.-P., KENNEDY, A.K., LI, Y. & DING, J. 2002b. SHRIMP U–Pb zircon geochronological and geochemical evidence for Neoproterozoic arc-magmatism along the western margin of the Yangtze Block, South China. *Earth and Planetary Science Letters*, **196**, 51–67.

Received 18 August 2003; revised typescript accepted 4 March 2004.
Scientific editing by Sally Gibson